Direct observation of homoclinic orbits in human heart rate variability

J. J. Żebrowski[1] and R. Baranowski[2]
[1]*Faculty of Physics, Warsaw University of Technology, Warszawa, Poland*
[2]*National Institute of Cardiology, Warszawa, Poland*

(Received 13 November 2002; revised manuscript received 18 February 2003; published 23 May 2003)

Homoclinic trajectories of the interbeat intervals between contractions of ventricles of the human heart are identified. The interbeat intervals are extracted from 24-h Holter ECG recordings. Three such recordings are discussed in detail. Mappings of the measured consecutive interbeat intervals are constructed. In the second and in some cases in the fourth iterate of the map of interbeat intervals homoclinic trajectories associated with a hyperbolic saddle are found. The homoclinic trajectories are often persistent for many interbeat intervals, sometimes spanning many thousands of heartbeats. Several features typical for homoclinic trajectories found in other systems were identified, including a signature of the gluing bifurcation. The homoclinic trajectories are present both in recordings of heart rate variability obtained from patients with an increased number of arrhythmias and in cases in which the sinus rhythm is dominant. The results presented are a strong indication of the importance of deterministic nonlinear instabilities in human heart rate variability.

DOI: 10.1103/PhysRevE.67.056216 PACS number(s): 05.45.−a, 82.40.Bj, 95.10.Fh

I. INTRODUCTION

Since its first description by Shilnikov [1,2] in 1965, homoclinic chaos, in which competition occurs between several unstable states including a saddle focus or a hyperbolic saddle, remains of interest. Chaos of this kind has been found in many systems, notably in hydrodynamic instabilities [3], in chemical reactions [4], in the dynamics of food chains [5], in laser dynamics [6–8], and in spiking phenomena [9]. The gluing bifurcation is also a characteristic feature of homoclinic chaos [10,3]. Synchronization in homoclinic chaos has been recently achieved—pursued mainly in the context of systems of neurons [11,12]. The paper by Postnov *et al.* [12] discusses coupled van der Pol oscillators as models of neurons. It was found that the interaction of the trajectory of the system with a hyperbolic saddle close to the homoclinic bifurcation may lead to a dephasing of synchronization. Van der Pol oscillators have been used since 1926 [28] to model the interaction of the natural pace-maker structures within the human heart (the sinus and the atrioventricular node).

The outstanding feature of homoclinic chaos is that the shape of the trajectories is very regular but the first return times (the time between subsequent crossings of a Poincaré section) may fluctuate strongly [13]. Consequently, return time maps are considered a tool of choice for the analysis of homoclinic chaos [14,8].

An electrocardiogram trace [15] is a recording of the electrical activity of the heart from electrodes on the surface of the body. It is composed of repeating shapes that do not differ much from each other over long periods of time. The shape of the trace is so typical that the extrema of the repeating spikes have been assigned the letters *P*, *Q*, *R*, *S*, and *T* with the *P* peak associated with the contraction of the heart atria and the *R* peak is associated with that of the ventricles. The RR interval then is the time between heartbeats. The RR interval may also be treated as the time of flight between Poincaré sections of the trajectory of the full ECG (see, e.g., Fig. 4.4.6 in Ref. [16]). It is well known that the heart rate fluctuates (a phenomenon called heart rate variability [15,17,16]) and that the origin of these fluctuations is not fully understood. The character of the heart rate variability is important for medical diagnostics and especially for the prediction of the risk of sudden cardiac death. Consequently, a large research effort has been made to establish that the source of the fluctuations is due to stochastic phenomena [18] or that they are due to nonlinear instabilities in a deterministic system [19,20]. One spectacular approach was the application of a modified OGY algorithm to the control of heart rate variability both in animal heart preparations as well as in humans [21]. Recently, however, these results as proof of the deterministic origin of heart rate variability have been disavowed by the work of Christini and co-workers [22,23], where it was found that the control algorithm works just as well for a system with noise and without a fixed point at all.

We have often found [24–26] that, in a three-dimensional projection in delay coordinates with the Takens delay equal to two heartbeats, the phase trajectory of the RR intervals is dominantly of two forms. In most healthy individuals, the RR intervals form a spiral trajectory repeatedly approaching the focus and diverging from it at an oblique angle. Such behavior is well known in systems where motion around a saddle focus occurs (compare, e.g., [9,8]). When the average heart rate changes, the focus shifts; but, otherwise, the topology of the trajectory remains the same. A crosslike shape, which we initially called radial behavior, was found to be associated with the pathological rather than the healthy heart rate variability. It may, however, also be found in some individuals considered to be healthy. It is the purpose of this paper to examine in detail the latter kind of RR interval trajectory using two-dimensional mappings. We examine three chosen cases of 24-h recordings of the heart rate variability (RR interval time series) in different patients. These datasets were chosen as representative but we have found the phenomena discussed below in many (over a hundred) other cases. We show that, if one investigates the second or fourth iterates of the RR interval map, homoclinic trajectories associated with flip saddles may be found—in some cases lasting many thousand heart beats. We find three different types of

these homoclinic trajectories and discuss whether the existence of such dynamics may be associated with arrythmia only or can be a signature of the properties of the sinus rhythm. The sinus node is the natural pacemaker of the heart. The findings of this paper are a strong indication of the importance of nonlinear instabilities in heart rate variability processes.

II. DATA

Heart rate variability data were extracted from 24-h Holter device ECG recordings using the 563 Del Mar Avionics system at the National Institute of Cardiology (Warszawa, Poland). All data were checked by a qualified cardiologist: normal beats were detected, artifacts were deleted, and arrhythmias were recognized. The data were sampled at 256 Hz except for an older recording (LCH), which was sampled at 128 Hz. The true error of automatic *R*-peak discrimination may be much larger than the nominal sampling error due to the distorted morphology of the QRS complex in severely ill patients. Then the error may be as large as 30 ms.

In over a hundred of the recordings in our database, homoclinic orbits were found. For this study, three demonstrative 24-h ECG recordings were chosen.

The patient LCH exhibited an extreme number of arrhythmic beats (over 70%) during the 24-h recording. The standard deviation of the RR intervals was very large (286 ms) but we have shown elsewhere [25] that, in fact, the data contain predominantly periodic orbits. It is the nature of these orbits which is the focus of the present paper.

The patient NRGLL had atrial flutter—a heart rhythm in which periodic electric activity at the atria occurs with a varying conduction to the ventricles. The RR intervals, in this condition, often appear as multiples of the basic period of atrial activity.

The patient SWK was characteristic: the standard deviation of heart rate variability was extremely low (55.6 ms) and there were less than 1000 ventricular arrhythmic beats in 24 h. This is then a case of sinus rhythm with a decreased heart rate variability.

III. RESULTS AND DISCUSSION

For each case, we examined the two-dimensional mappings of RR$(i+\tau)$ versus RR(i). i is the RR interval index and τ denotes the iterate of the map. We changed τ from 1 to 6 for all cases studied but the most interesting results were obtained for the second and the fourth iterate of the RR interval maps.

The first case we examine here is that of patient LCH—since deceased. In the 24-h ECG recording, over 70% of heartbeats were due to ventricular arrhythmia. The complete heart rate variability record is presented in Fig. 1. It has been shown elsewhere [25] that this patient—in spite of an extremely large variance of the RR intervals (286 ms)—exhibited period-3 orbits for the best part of the 24-h recording (with only occasional occurrences of period-5 or higher orbits; there were also some narrow periods of the time of extremely low variance but with an irregular heart rate).

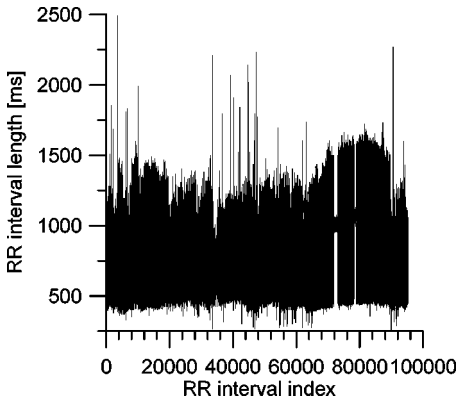

FIG. 1. 24-h long recording of heart rate variability for the LCH case: RR intervals as a function of the interval index.

We focus on a portion of the recording depicted in Fig. 2—it can be seen that large excursions of the RR interval value are interspersed with a low variance heart rhythm. In fact, LCH is one of the two recordings that inspired the search for type-I intermittency in heart rate variability [27]. Let us examine in detail how does a given RR interval map onto the next one. Figure 3 depicts a sequence of 260 evolutions of the system starting at RR interval index $i=76\,400$ and presented as the map RR$(i+1)$ vs RR(i). It can be seen that the data points form a trajectory resembling a period-3 orbit with noise or what seems to be drift along the diagonal interposed on it. This drift spans only ≈ 200 ms along the diagonal and is consistent with all our earlier observations [24,26,25] that—for a given person—the topology of the trajectory of the RR interval in delay coordinate space stays constant for very long periods of the time. It is only the center of gravity of the trajectory that moves along the diagonal reflecting the change of average heart rate. In Fig. 3 it can be seen that the RR intervals left the periodic trajectory for only 3 out of the 262 evolutions shown.

To understand better the nature of the trajectory of RR intervals for this case, we will examine the second iterate (Fig. 4). The 262 RR intervals form a cross-shaped trajectory with some of the RR intervals close to the diagonal. Only when one patiently follows through the evolution of the trajectory in Fig. 4, it becomes evident that it is formed of a

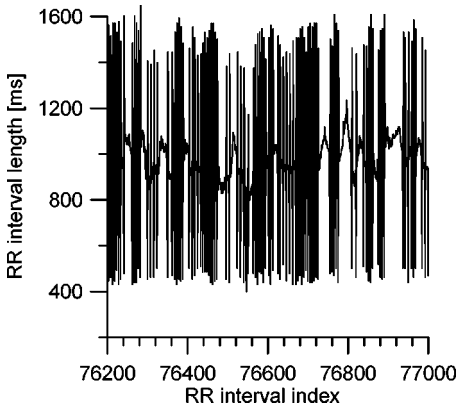

FIG. 2. Short fragment of the data in Fig. 1.

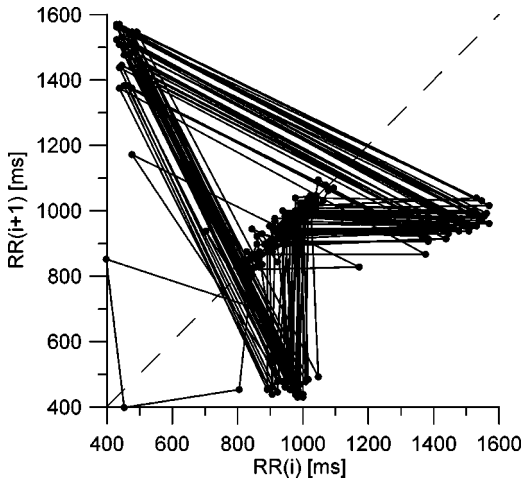

FIG. 3. Return map of the data in Fig. 2.

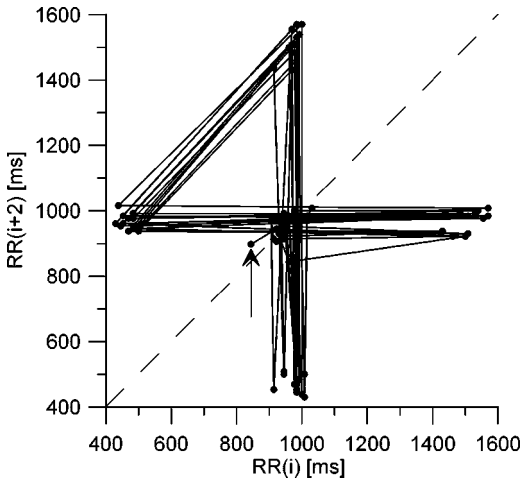

FIG. 5. A fragment of the trajectory of Fig. 4: RR interval index $i = 76\,400–76\,477$. The arrow marks the last point.

single, somewhat noisy hyperbolic saddle point to which the trajectory returns repeatedly. Figure 5 depicts the first part of the trajectory associated with the saddle point—originating at a location very close to the fixed point and ending at the arrow (RR index $i = 76\,400–76\,477$). Twelve homoclinic branches of the trajectory may be seen in this figure. The width of the spread of the location of the points on the diagonal is less than 80 ms.

Figure 6 depicts the next sequence of events starting at $i = 76\,477$ and ending at $i = 76\,510$. At the beginning of this sequence, the average heart rate drops slightly and the trajectory remains close to the diagonal. This behavior has all the features of a slightly noisy nodal point (19 data points with standard deviation 28.5 ms) gradually drifting upwards along the diagonal. Then, in a region that lies at the lower border of the saddle seen in Fig. 5, again trajectories along portions of the unstable and stable manifolds are seen with just two branches of the homoclinic orbit. At the end of the sequence (filled arrow in Fig. 6), the trajectory lands above saddle point and is allowed to linger close to the diagonal for several heartbeats. In the time that follows, until a major change of the average heart rate occurs so that the system leaves this part of the phase space, the trajectory will become affected by the stable and unstable manifolds repeatedly (Fig. 7 for $i = 76\,510–76\,650$). The case of LCH is special in the sense that this patient exhibited an extremely large standard deviation of the heart rate (286 ms; Fig. 1) but the average heart rate stayed approximately constant for extended periods of time (the 24-h average of the RR intervals was equal to 832 ms).

The homoclinic trajectory discussed in Figs. 4–7 was found throughout the LCH recording and it is very common in the recordings of heart rate variability examined by our group. Whenever it occurred for the LCH case, the position of the saddle shifted by less than ± 50 ms and it was obtained in the range of RR interval length between 650 and 1000 ms. The most often obtained position was at 720–750 ms, at 900 ms and at 1020 ms. In particular, at the latter position, the saddle point was obtained for index i between 77 760 and 80 680 with its position fixed at 1020 ms ± 40 ms.

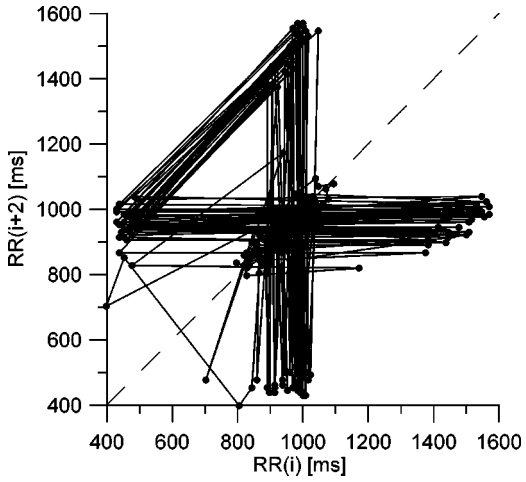

FIG. 4. Second iterate of the map in Fig. 3: the RR interval index i changes from 76 400 to 76 650.

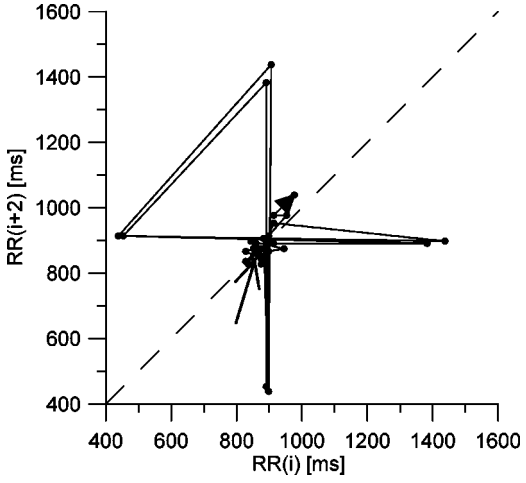

FIG. 6. The next fragment of the trajectory of Fig. 4: index $i = 76\,477–76\,510$. The lower arrow marks the beginning and the upper arrow marks the end.

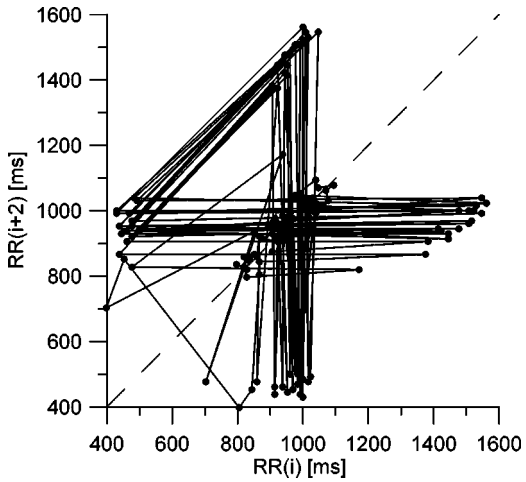

FIG. 7. The last fragment of the trajectory of Fig. 4: index $i = 76\,510–76\,650$. The saddle point shifts by about ± 50 ms.

Two other homoclinic orbits were found in the LCH recording. One was obtained uniquely for RR intervals between $i = 8400$ and $i = 10\,150$ for the map RR$(i+4)$ vs RR(i). It is a much more complex homoclinic trajectory. In Fig. 8, which depicts a fragment of this trajectory for RR intervals from the range of the index from 8930 to 9030, the stable and unstable directions of the saddle point may be distinguished but the evolution between these manifolds is more complex than discussed before. In the whole range, in which this kind of homoclinic trajectory was found, the position of the saddle point was fixed between 900 and 950 ms.

The third kind of homoclinic trajectory was found only at the beginning of the recording. Figure 9 depicts a particularly long example of this kind—obtained for RR interval index $i = 2640–2880$. It can be seen that the trajectory contains three rotations of a period-3 orbit but otherwise the image is consistent with a hyperbolic saddle situated at 725 ± 25 ms. The important difference in Fig. 9 as compared to the homoclinic orbits discussed above is that, in this case, there are no RR intervals that land at the diagonal. This type

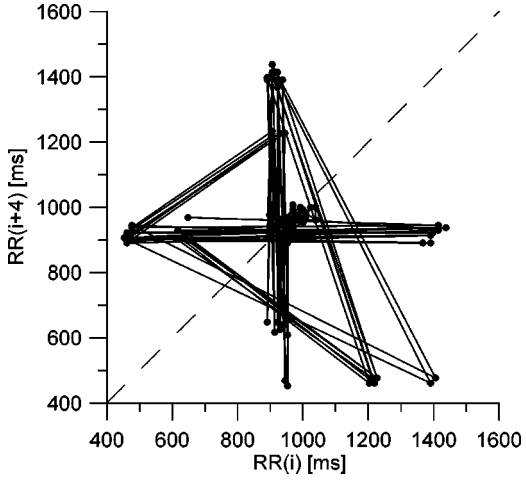

FIG. 8. The fourth iterate of the RR interval map for $i = 8930–9030$. This is a fragment of a 1750-interval-long trajectory.

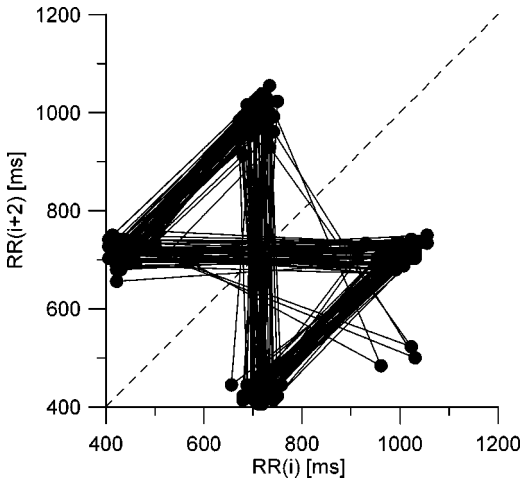

FIG. 9. The second iterate of the map of RR intervals for $i = 2640–2880$. The trajectory may be the result of a gluing bifurcation: note the lack of data points on the diagonal.

of orbit may occur at a gluing bifurcation (e.g., compare Fig. 4 of Ref. [10]) In our measurements, it was obtained rarely and only for much shorter periods of time than the other two kinds found for the patient LCH.

All unstable fixed points discussed up to now have been of the flip saddle kind. Although this kind of saddle seems to be the easiest to find in heart rate variability time series, it is not always the case. Figure 10 depicts 250 consecutive RR intervals projected as a second iterate map for the patient NRGLL who had permanent atrial flutter. It can be seen that the trajectory of the system remains on one side of the fixed point moving along the unstable and the stable direction consecutively (note the enlarged scale of Figs. 10 and 11 below) and that the position of the saddle point remains stable within ± 25 ms. Such a shape of the trajectory may occur above the gluing bifurcation (see Fig. 4 of Ref. [10]). The

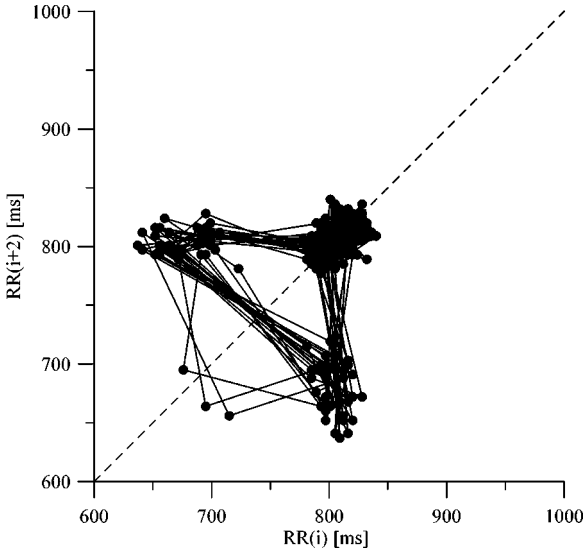

FIG. 10. Second iterate of the RR interval map (250 intervals) for the NRGLL case. Another example of a possible result of the gluing bifurcation.

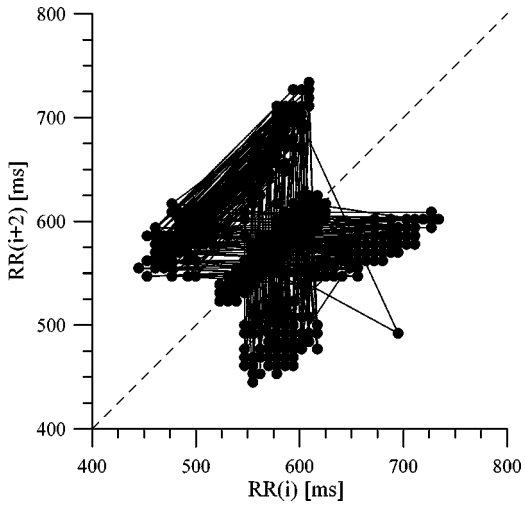

FIG. 11. Homoclinic trajectory for a case (SWK) with sinus rhythm (9500 consecutive intervals, i.e., 1.5 h).

kind of behavior depicted in Fig. 10 is also very common among the different heart rate variability cases studied by our group.

All instances of homoclinic orbits discussed above have been obtained in cases where different kinds of arrhythmia were abundant. However, saddle points may be obtained also—if somewhat more rarely—for cases of prevalent sinus rhythm. The patient SWK was special: the standard deviation of the heart rate was extremely low (56 ms) and there were less than 1000 ventricular arrhythmic beats during 24 h. And yet a well formed homoclinic orbit associated with a period-2 flip saddle may be found in this case for long periods of the time. Figure 11 depicts an example—found for RR interval index $i=1-9500$ (note the changed scale of the figure). It can be seen that the position of the saddle itself fluctuates by not more than ± 30 ms, which is within the upper bounds of the error of the automatic heart rate variability analysis algorithm of the Holter device. Thus, for a long time (the 9500 RR intervals corresponded to about 1,5 h) the saddle point remained at one position. For $i=9500-10\,440$, a fixed point (a node) slowly drifting upwards along the diagonal was obtained and for $i=10\,440-19\,952$ again the same homoclinic orbit as seen in Fig. 11 was obtained. Note that, during this long time, in this case the saddle point drifted between 550 ms and 670 ms. Similar behavior was obtained also for $i=31\,350-33\,369$, $34\,000-55\,000$ (saddle point at 550–650 ms), $55\,000-73\,650$ (saddle point at 650–750 ms). Within $i=73\,650-101\,257$ a fixed point was found drifting between 650 and 750 ms and, finally, for $i=101\,257$ till the end of the recording at $i=127\,928$ again a homoclinic orbit was found. Within this time the saddle point drifted from ≈ 700 ms to a position at about 570 ms.

We do not have a model that reproduces the type of behavior presented above. The van der Pol oscillator and its modifications have been used in the past [28–31] to model the properties of the sinoatrial node and of the atrioventricular node. There seems to be a consensus among physiologists that these nodes may be treated as coupled oscillators and that they interact with at least a third oscillator—the baroreceptor system (quite possibly there may be as many as nine interacting oscillators in the whole system if one also considers the various areas of the heart that may be a source of arrhythmia). In addition, we have the moderating effect of the autonomic nervous system on the properties of the heart rate. We are dealing with a very complex system.

One question that should be discussed in the context of the results of our measurements is whether one may interpret the trajectories as a persistent saddle point in spite of the fact that the system—at least in principle—is nonstationary. After all, the Holter ECG is a portable device and the subjects were free to follow their daily activities and were not constrained to some well defined (stationary) behavior. Assuming that one may judge by the properties of a single van der Pol system, we made a simulation using the XPP system [32] with the modified van der Pol system of Ref. [12]. In this model, it is possible to change the position of the stable node, of the hyperbolic saddle, and the properties of the limit cycle in a wide range. Moreover, the position of these points may be set to a large degree independently. In our simulation, the position of the saddle point was modified harmonically with the time at a frequency 1.5 times the natural limit cycle frequency of the oscillator. The amplitude of the motion of the saddle was chosen in such a way that the saddle repeatedly approached the limit cycle stopping just before the homoclinic bifurcation occurred. If the bifurcation would have had occurred, the state point would have moved from the limit cycle to the stable node [12]. The time between zero crossings was determined for each movement around the limit cycle and a mapping of these times was constructed. It was found that the limit cycle is stable against such parametric perturbation. In the third iteration of the mapping, a node drifting back and forth along the diagonal was obtained. This motion of the node is equivalent to a change in the frequency of the limit cycle. In this simple model, we did not obtain a destabilization of the limit cycle (which should lead to a saddle visible in the mapping). Note, however, that, occasionally, in our measurements there also appears a node sliding along the diagonal. We stress that the only reason we made the simulation was to see if the van der Pol system—a good candidate for use in future modeling of our results—will yield a behavior structurally stable under such a parametric nonstationarity close to the homoclinic bifurcation. The model used in the simulation is, however, much too simple to provide results fully resembling what we see in our measurements.

In the past, attempts have been made to find stable and unstable manifolds in heart rate variability—notably Ref. [21] and references therein. The main differences between the results published earlier and our results are the following.

(1) Other authors endeavored to find the stable and unstable directions based on just a small number of evolutions of the system while here we show many hundreds or even thousands of occurrences of consecutive, repeated behavior, which is found to be extremely persistent in the time.

(2) To our knowledge, no other group tried to look for fixed points in higher-order mappings of the RR intervals—they restricted themselves to $\mathrm{RR}(i+1)$ vs $\mathrm{RR}(i)$.

IV. CONCLUSIONS

Maps of consecutive RR intervals (iterates of such maps from the first to the sixth) for three medically characteristic cases were examined. Homoclinic orbits associated with several different period-2 and period-4 hyperbolic saddles were found. Prevalently, these hyperbolic saddle points were of the flip kind and features typical for a gluing bifurcation were obtained in some cases. For a given patient, the phenomena observed may be heart rate dependent, as saddle points were found to occur repeatedly in specific ranges of the heart rate.

Although the hyperbolic saddle points may readily be found in the heart rate variability of patients with arrhythmia, the same kind of homoclinic orbit may be found in patients with a dominantly sinus rhythm. This seems to be an important finding. It indicates that the source of the variability of the heart rate may be due to the instabilities of the sinus node and the systems that control it. Arrhythmia seems to enhance the ability of the system to form homoclinic orbits as it is much easier to find such a behavior in patients with arrhythmia. On the other hand, it is not only of purely physical but also of medical interest to investigate the relationship between arrhythmia and the presence of homoclinic orbits. It is well known that arrhythmia *per se* is not always malignant and not in all the cases does it lead to cardiac arrest (i.e., to sudden death). Whether the presence or the absence of homoclinic orbits as well as their stability or instability is the modulating or the determining factor, is a subject for future research.

The existence of homoclinic orbits and the very little spread in the position of the saddle points for sustained periods of time indicate the importance of deterministic instabilities in the heart rate regulation precesses. Note also that, in view of the similarity of the morphology of the QRS complex from heartbeat to heartbeat—a similarity which is also an important feature of oscillations in Shilnikov chaos—future research work may show that the complete ECG is also a result of homoclinic trajectories.

ACKNOWLEDGMENTS

The authors are very grateful to L. Glass and D. Kaplan for inspiring discussions. This work was supported by KBN Grant No. 5 P03B 001 21. A. Krawiecki is thanked for a critical reading of this paper and K. Grudziński for making the simulation.

[1] L.P. Shilnikov, Sov. Math. Dokl. **6**, 163 (1965).
[2] *Homoclinic Chaos*, *NATO Advanced Research Workshop* [Physica D **62** (1–4) (1993)].
[3] J.M. Lopez and F. Marques, Phys. Rev. Lett. **85**, 972 (2000).
[4] A. Arneodo, F. Argoul, J. Elezgaray, and P. Richetti, Physica D **62**, 134 (1993).
[5] B.W. Kooi, M.P. Boer, and S.A. Kooijman, Math. Biosci. **153**, 99 (1998).
[6] S. Wieczorek, B. Krauskopf, and D. Lenstra, Phys. Rev. Lett. **88**, 063901 (2002).
[7] H.J. Wünsche, O. Brox, M. Radziunas, and F. Henneberger, Phys. Rev. Lett. **88**, 023901 (2002).
[8] A.N. Pisarchik, R. Meucci, and F.T. Arecchi, Eur. Phys. J. D **13**, 385 (2001).
[9] R. Meucci, A. Di Garbo, E. Allaria, and F.T. Arecchi, Phys. Rev. Lett. **88**, 144101 (2002).
[10] D. Pazo and V. Pérez-Muñuzuri, Phys. Rev. E **64**, 065203(R) (2001).
[11] E. Allaria, F.T. Arecchi, A. Di Garbo, and R. Meucci, Phys. Rev. Lett. **86**, 791 (2001).
[12] D. Postnov, S.K. Han, and H. Kook, Phys. Rev. E **60**, 2799 (1999).
[13] F.T. Arecchi *et al.*, J. Opt. Soc. Am. B **5**, 1153 (1988).
[14] A.R. Zeni, T. Braun, R.R.B. Correia, P.Jr. Alcantara, L. Guidoni, and E. Arimondo, Phys. Rev. E **57**, 288 (1998).
[15] D. P. Zipes and J. Jalife, *Cardiac Electrophysiology: From Cell to Bedside* (Saunders, Philadelphia, 2000).
[16] B. J. West, *Fractal Physiology and Chaos in Medicine* (World Scientific, Singapore, 1990).
[17] L. Glass and M. C. Mackay, *From Clocks to Chaos: The Rhythms of Life* (Princeton University Press, Princeton, 1988).
[18] A.L. Nunes Amaral, A.L. Goldberger, P.C. Ivanov, and H.E. Stanley, Comput. Phys. Commun. **121-122**, 126 (1999).
[19] *Nonlinear Analysis of Physiological Data*, edited by H. Kantz, J. Kurths, and G. Mayer-Kress, Springer Books on Synergetics (Springer, Berlin, 1998).
[20] N. Marwan, N. Wessel, U. Meyerfeldt, A. Schirdewan, and J. Kurths, Phys. Rev. E **66**, 026702 (2002).
[21] W.L. Ditto *et al.*, Int. J. Bifurcation Chaos Appl. Sci. Eng. **10**, 593 (2000).
[22] D.J. Christini and J.J. Collins, Phys. Rev. Lett. **75**, 2782 (1995).
[23] D. Kaplan (unpublished).
[24] J.J. Żebrowski, W. Popławska, and R. Baranowski, Phys. Rev. E **50**, 4187 (1994).
[25] J.J. Żebrowski, W. Popławska, R. Baranowski, and T. Buchner, Chaos, Solitons Fractals **11**, 1061 (2000).
[26] J.J. Żebrowski, W. Popławska, R. Baranowski, and T. Buchner, Acta Phys. Pol. B **30**, 2547 (1999).
[27] J.J. Żebrowski, Acta Phys. Pol. B **32**, 1531 (2001).
[28] B. van der Pol and J. van der Mark, Philos. Mag. **6**, 763 (1928).
[29] B.J. West, A.L. Goldberger, G. Rowner, and V. Bhargava, Physica D **17**, 198 (1985); B.J. West, A.L. Goldberger, J. Mandelli, and V. Bhargava, *ibid.* **17**, 207 (1985).
[30] O. Kongas, R. van Hertzen, and J. Engelbrecht, Chaos, Solitons Fractals **10**, 119 (1999).
[31] D. di Bernardo, M.G. Signorini, and S. Cerutti, Int. J. Bifurcation Chaos Appl. Sci. Eng. **8**, 1975 (1998); M.G. Signorini, S. Cerrutti, and D. di Bernardo, *ibid.* **8**, 1725 (1998).
[32] The XPP package is available at http://www.math.pitt.edu/~bard/xpp/xpp.html